HISTORIA NATURAL

Tercera Serie | Volumen 12 (3) | 2022/5-19

RAMAN SPECTROSCOPIC ANALYSIS OF DIAMONDS AND ITS MINERAL INCLUSIONS FROM "LAMPROITES" IN THE CAPIIBARY, SAN PEDRO DPTO., PARAGUAY

Análisis Espectroscópico Raman de Diamantes y sus Inclusiones Minerales de "Lamproitas" junto a la ciudad de Capiibary, Departamento de San Pedro, Paraguay

Jaime L.B. Presser[1] and Arif M. Sikder[2]

[1]JP-Explorations, Asunción – Paraguay. presserjaime@gmail.com

[2]Center for Environmental Studies (CES), Virginia Commonwealth University (VCU) amsikder@vcu.edu

AZARA
FUNDACIÓN DE HISTORIA NATURAL

umai Universidad Maimónides

Abstract. The diamond in Paraguay was reported for the first time in 1825, and around 1960 the first artisanal exploitation was carried out in the city of Capiibary, Department of San Pedro, Eastern Paraguay. The first scientific analysis of Capiibary diamonds was conducted in 2012. A set of millimeter-sized new crystals of Capiibary diamonds from cratonic lamproite colluvium/alluvium with a higher abundance of inclusion were selected for Raman spectroscopic analysis of the diamonds and their mineral inclusions. The selected set of diamond crystals is transparent brown, light-brown, cognac brown, colorless to colorless with a faint yellow tint, and green to shades of green. The crystals are sharp axes octahedral (some with polycentric development of the crystalline faces) or with partially reabsorbed rounded octa-dodecahedral transition forms; pseudo hemimorphic form and also crystals with irregular rounded shapes; whole to fractured crystals. Raman spectra obtained from the majority of the studied crystals, except one, exhibit an explicit change of D-peak wavenumber (shifts from 1294 to 1353 cm^{-1}) and variable FWHM numbers (>>3 to 197 cm^{-1}) characteristic of diamond with internal defects, as observed in lonsdaleitic diamonds. The lonsdaleitic diamonds signature in the crystal structure of host diamonds associated with the suit of super deep inclusions (Ca-perovskite, bridgmanite, stishovite, and ferropericlase associations) support the conclusion that the Capiibary diamonds were probably derived from a source (subducted Nazca slab) situated in the lower mantle and transformed partially into lonsdaleite or mixed cubic hexagonal polytype structures of diamonds by a kinetic process of shear stress and the shock wave compression induced by provable very high temperature.

Keywords. Capiibary diamond Raman Spectroscopy, lonsdaleitic diamond, lower mantle diamond inclusions, diamond-bearing lamproite, Paraguay.

Resumen. El diamante en Paraguay fue reportado por primera vez en 1825, y hacia 1960 se realizó la primera explotación artesanal en la ciudad de Capiibary, Departamento de San Pedro, Paraguay Oriental. El primer análisis científico de los diamantes de Capiibary se realizó en 2012. Para el presente trabajo se seleccionaron un conjunto de nuevos cristales de diamantes de Capiibary ellos siendo de tamaño milimétrico, provenientes de coluvión/aluvión junto a un conducto de lamproita cratónica, con mayor abundancia de inclusiones minerales para el análisis espectroscópico Raman de los diamantes y de las inclusiones en ellos. Los cristales de diamante seleccionados son de color marrón transparente, marrón claro, marrón coñac, incoloros a incoloros con un leve tinte amarillo y verdes a tonos de verde. Los cristales siendo octaédricos de ejes agudos (algunos con desarrollo policéntrico de las caras cristalinas) o con formas de transición octa-dodecaédricas redondeadas parcialmente reabsorbidas; forma pseudo hemimorfa y también cristales con formas redondeadas irregulares; cristales enteros a cristales fracturados. Los espectros Raman obtenidos de la mayoría de los cristales estudiados, excepto uno, exhiben un cambio explícito del valor del pico-D (desplazamientos de 1294 a 1353 cm^{-1}) y valores de FWHM variables (>>3 a 197 cm^{-1}) característicos de diamantes con defectos, como observados en los diamantes lonsdaleíticos. La huella de diamantes lonsdaleíticos en la estructura cristalina de los diamantes anfitriones asociados con el juego de inclusiones súper profundas (asociaciones de Ca-perovskita, bridgmanita, stishovita y ferropericlasa) respaldan la conclusión de que los diamantes de Capiibary probablemente se derivaron de una fuente (placa de Nazca subductada) situada en el manto inferior y que se transformó parcialmente en lonsdaleita o estructuras de politipo hexagonal-cúbico mixto de diamantes por un proceso cinético de esfuerzo cortante y la compresión de ondas de choque inducidas por eventuales temperaturas muy altas.

Palabras clave. Espectroscopia de Raman de diamantes de Capiibary, diamante lonsdaleitico, inclusiones de diamante del manto inferior, lamproitos con diamantes, Paraguay.

INTRODUCTION

The history of diamond discovery in Paraguay goes back to early 1825 (Aimé Bonpland, in Santa Maria, Dpto. Misiones, in Presser, 2019a), but artisanal exploitation started only in the 1960s around the city of Capiibary, Department of San Pedro, Eastern Paraguay (Figure 1). Diamond and diamond-bearing cratonic lamproites are located in the Eastern Paraguay Ultrapotassic Province (Smith *et al.*, 2012; Presser *et al.*, 2014a; Presser *et al.*, 2014b; Presser *et al.*, 2017; Presser, 2016; and Presser, 2019a).

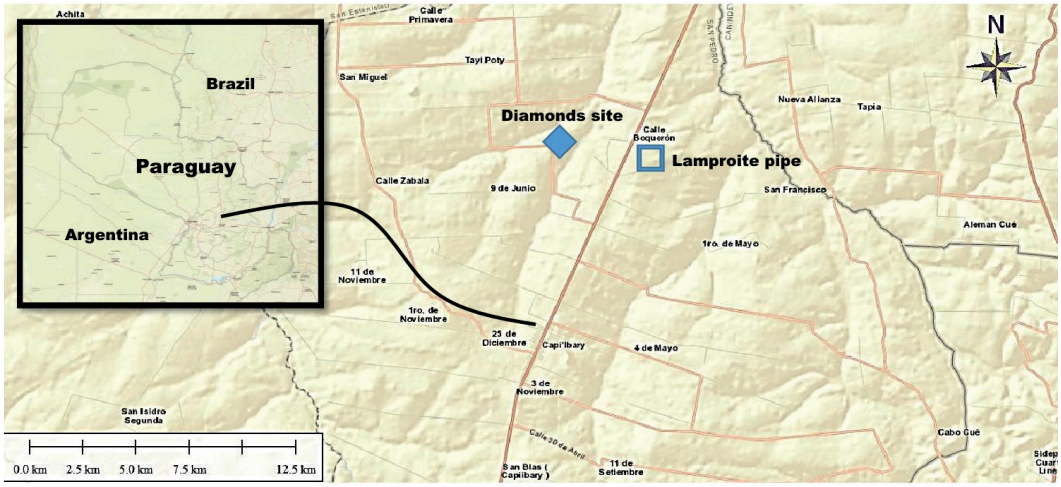

Figure 1 - Diamonds from stream placers/colluvium deposits adjacent to cratonic lamproite pipe anomaly of Capiibary area (top of figure).

Very little scientific information on the Capiibary diamonds is available. Recently, the alluvial Capiibary diamonds were systematically analyzed concerning their external morphology, nitrogen content, and aggregation (Smith *et al.*, 2012; Presser *et al.*, 2014b). Still to date very little emphasis is given to the identification of the mineral inclusions of Capiibary diamonds to understand their depth of origin in the mantle.

A batch of Capiibary diamond crystals with a higher abundance of inclusions (Figure 1) is selected for the present study. Eleven [11] crystals, out of the new batch of diamonds, were utilized for detailed Raman spectroscopic analysis and the results of the analysis are presented to illustrate the probable origin of Capiibary diamonds.

MATERIALS AND METHODS

Twenty [22] millimeter sizes (1 to 3 mm) diamonds were collected for the present study from the alluvion/colluvium deposits adjacent to the lamproite pipe anomaly of Capiibary city (Figure 1). The pipe anomaly was discovered about 3.5 kilometers from the diamond-bearing olivine lamproite pipe (Presser *et al.*, 2017; Presser, 2016; Presser, 2019a; Presser and Benítez, 2021) (Figure 1). Most of the studied diamond crystals are transparent and range in color from brown to light brown and cognac brown, colorless to colorless with a faint yellow tint, and green to shades of green. Euhedral crystals are octahedral and some of the diamonds are with faces of polycentric development of crystals. There are also crystals with rounded partially resorbed octa-dodecahedral transition shapes and pseudo hemimorphic form (usually associated with recent derivation from mantle xenoliths) to an irregular whole to fractured crystals and crystals with irregular round shapes. In some of these diamonds, green radiation damage spots and brown radiation spots are also present (Figures 1 and 2).

Raman spectra were obtained from eleven [11] selected diamonds and the mineral inclusions in the range from 100 to 1800 cm $^{-1}$, with a 300-second acquisition time, by using the Horiba LabRAM HR Evolution Confocal micro-Raman spectrometer with a 20 mW, 532 nm He-Ne- laser excitation system, a grating with 600 grooves/mm, and a thermoelectrically cooled CCD array detector at the Nanomaterial Core Characterization Facility (NCCF) of Virginia Commonwealth University (VCU), USA. Long working distance lenses at 100×, 50×, or 10× magnification, were used for permitting analysis of inclusions as deep as a few millimeters.

Raman spectra were processed using the two open-source software. CrystalSleuth (https://rruff.info) was used to remove the background noise for enabling the comparison of multiple spectra and Spectragryph was used for deriving individual peak values, full width at half maximum (FWHM) calculation, and Gaussian deconvolution of the spectrums.

RESULTS AND DISCUSSIONS

To know the spectral characteristics of Capiibary diamonds and to determine the mineral phases of the inclusions, 150 Raman spectra from 11 selected crystals of diamond were obtained. In the defect-free cubic natural diamonds, the most intensive wavenumber position of the Raman spectrum is 1332.5 cm^{-1} (Zaitsev, 2013; Green *et al.*, 2022), i.e. D-peak, and any shift to either higher or lower than this wavenumber would have genetic implications or suggesting crystal disorder or crystal defects (*cf*. Miyamoto *et al.*, 1993; He *et al.*, 2002; Goryainov *et al.*, 2014; Jones *et*

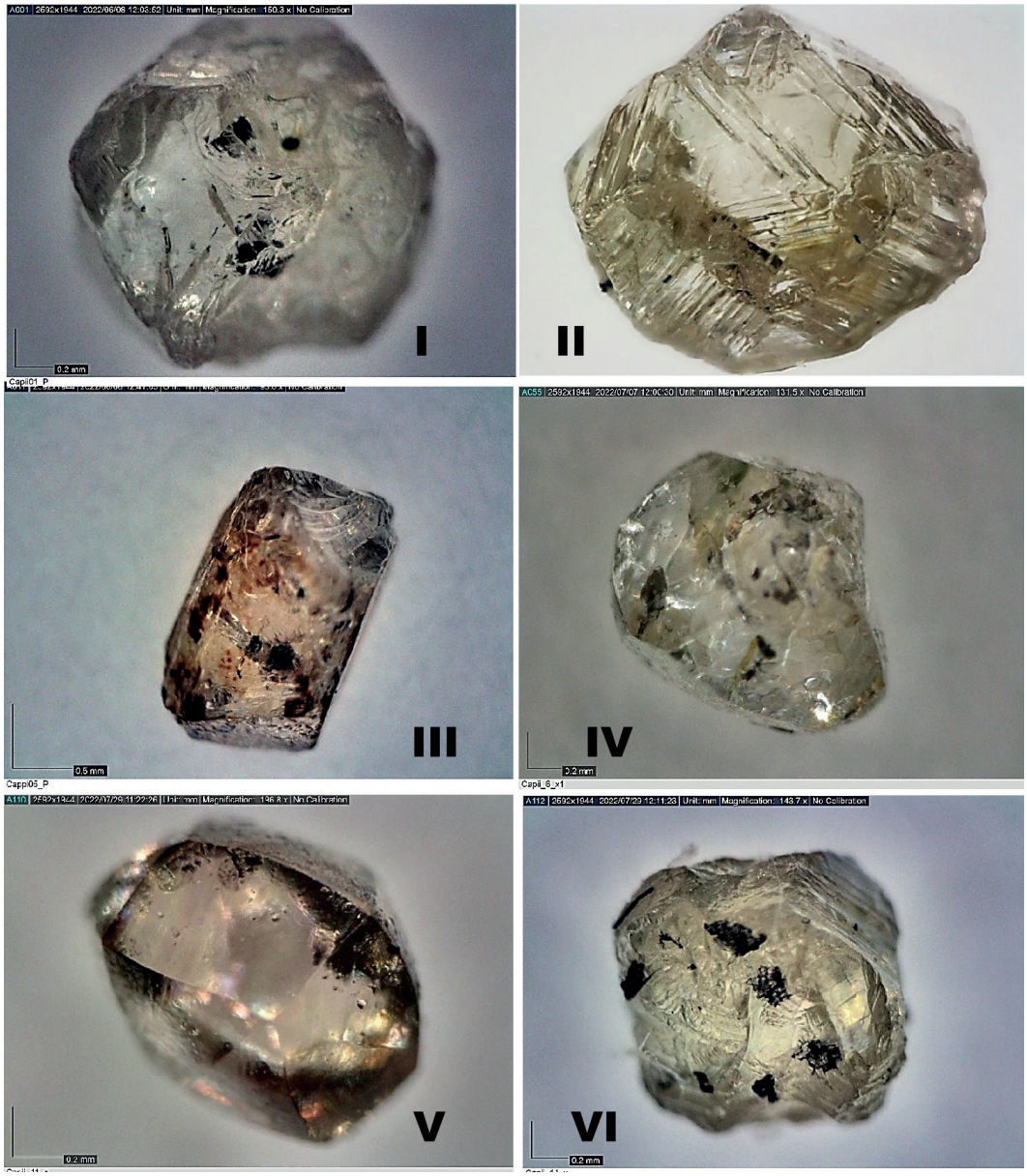

Figure 2 - Photos of 6 diamonds rich in inclusions study of the 13 selected diamond crystals pointed to the recognition of the Raman spectrum. I, Capii-1; II, Capii-3; III, Capii-5; IV, Capii-6; V, Capii-10; and VI, Capii-14.

al., 2016; Di Liscia, *et al*., 2013 and Presser *et al*., 2020). Most of the Raman spectra of the host diamonds in the present study (11 out of 13) show an unusual variation in the D-peak intensity and shift in D-peak position, i.e. lower or higher than the D-peak wavenumber (Figure 3A). Only one crystal with a peak at ~1332 cm^{-1} (Capii-2) was recorded in the present analysis. The rest of the samples show D-peaks of either low or

high wavenumber than 1332.5 cm^{-1} (Table 1) Moreover, the discrepancy in the Capiibary diamond D-peak intensity and shift in D-peak position observed in the same crystal could indicate that the diamonds would possess some crystal defects (Figure 3A and B).

Raman spectra (n=42) of one of the Capiibary diamonds (i.e. Capii-6) show wide variation in D-peak wavenumber between 1313.3 and 1353.4 cm^{-1}, consisting of D-peak (I), low-quality diamond peak (II) and G-peak or graphite peak (III) (Figure 3B). If the Raman spectrum shows a peak at wavenumber ±1450 cm^{-1} representing the low-quality diamond, suggesting that this Capiibary diamond crystal is probably with structural defects. The intense G-peak is due to the presence of graphite as inclusion (wavenumber ±1600 cm^{-1}). Also, we recognized crystals with wavenumber peaks at ~1294 to 1347 cm^{-1} (Capii-1, Capii-3, Capii-5, Capii-7, Capii-8, Capii-10, Capii-14, Capii-16 and Capii-17). Table 1.

One of the diamond spectrums of Capii-6-29 (Figure 3) exhibits a prominent and wide peak in D-zone (wavenumber 1342 cm^{-1} and FWHM: 117.9 cm^{-1}) followed by another notable peak in G-zone (wavenumber 1607 cm^{-1}). FWHM of the defect-free cubic diamonds is generally ~3 cm^{-1} in D-zone. Whereas FWHM of the D-zone of several crystals of the present study shows a RAW high value greater than 5 cm^{-1} (Ta-

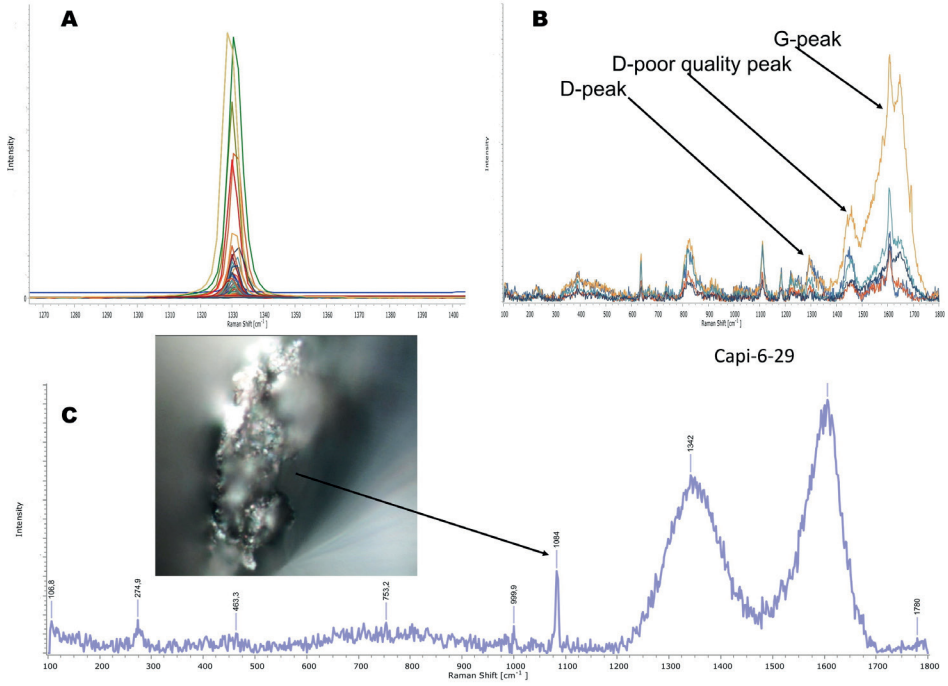

Figure 3 - Typical Raman spectra of Capiibary diamonds A, The Raman spectrum of Capiibary diamonds show different intensities and shifting D, bands. B, the spectrum obtained from Capii-6 diamond shows the diamond peaks (Peak D), low-quality diamond D peaks, and the G peak (graphite peak). C, Photomicrograph of calcite and the arrow points to the 1084 cm^{-1} peak of the calcite inclusion. Raman spectrum of one of the Capiibary diamonds (Capii-6-29) unexpectedly shows multiple peaks of variable wavenumber between 1313.3 and 1353.4 cm^{-1}. a peak at wavenumber ±1450 cm^{-1} that portrays the low-quality diamond and an intense G-band (±1600 cm^{-1}) due to the presence of graphite as inclusion, suggests that the diamond crystal has structural defects.

ble 1). So too, it should be noted that the D-peak wavenumber of seven spectra of Capii-1 ranges from 1294 to 1331.8 cm^{-1} and FWHM between 4.3 and 76 cm^{-1}; ~1330 cm^{-1} with FWHM 9-42.5 cm^{-1} in the Capii-14; and in the Capii-6, as commented above, were obtained in three Raman spectra FWHM 2.3-197 cm^{-1} Table 1. As already commented, the calculated FWHM from raw data in 10 out of 11 crystals shows a greater high value than 5 cm^{-1}; in this regard, for example, Qiu *et al.* (2004) noted that the FWHM in the diamonds increases with increasing pressure; which would be expressed as crystal disorder.

So, the crystal disorder in Capiibary diamonds can be indicated by deviations in the position of the D-peak wavenumber or by high to extremely high values in FWHM. Some readings with high FWHM values show the low intensity of the D-peak wavenumber while the typical peaks wavenumber of the D-peak is pronouncedly intense. Multiple deviations of D-peak wavenumber and FWHM (i.e., heterogeneity) were recorded in the same crystal¸ which may indicate that the diamond is obviously with some crystal defects.

Raman spectroscopic studies of the impact diamonds revealed the broadening and shifting of the D-peak position as an indication of the presence of lonsdaleite or mixed cubic hexagonal polytype structures (*cf*. Goryainov *et al*., 2014; Jones *et al*., 2016; Ovsyuk *et al*., 2019; Murri *et al*., 2019; Németh *et al*., 2022). In Raman spectral analysis of natural diamonds mainly was not focused on any crystal disorder yet (DeCarli *et al*., 2002) so overlooked the possibility of encountering any crystal disorder in the natural diamonds that occur in kimberlites, or lamproites, and in other diamond-bearing rocks of volcanic origin. But lonsdaleite or mixed cubic hexagonal polytype structures is already identified with some level of uncertainty in the diamonds from the Liaoning Deposit in China by Gorshkov *et al.* (1997); however, this does not appear to have had the necessary credibility (*cf*. Jones *et al*., 2016, and so as, Kaminsky, 2017). Though recently Wu *et al.* (2022) studies of the brown diamond from the Mengyin Kimberlite of China revealed dislocation and stacking faults in diamonds in TEM studies with corresponding Raman diamond peak between 1326 cm^{-1} to 1328 cm^{-1}; a shift in the diamond peak position (both, is a lonsdaleitic diamond's characteristics; as can be seen in Jones *et al*., 2016; Murri *et al*., 2019; Németh *et al*., 2022).

On the other hand, Smith *et al.* (2022) provides an instructive, academic, and very useful background on the determination of inclusions in diamonds via Raman spectroscopy (but see also Smith *et al*., 2017; Smith *et al*., 2018; Anzolini *et al*., 2018; Kemppinen, 2019; Zedgenizov *et al*., 2016; Zedgenizov *et al*., 2020; Thomson *et al*., 2014). However, not all the spectra were easy to treat due to their low-intensity wavenumber between 100 and 1200 cm^{-1}, a particular range for most inclusions of diamonds (Smith *et al*., 2022). Smith (2021) provides the material with a vast database of Raman spectra of lithospheric and sublithospheric inclusions in diamonds. To ascertain further the mantle origin of the Capiibary diamonds, the present study was also focused on determining the type of micron size inclusions of the 11 well-selected Capiibary diamond crystals with Micro Raman Spectroscopy.

In figure 2C a photo of inclusion is shown next to the spectrum of Capii-6-29; it would be calcite (strong characteristic peak wavenumber at 1084 cm^{-1}). In the sample Capii-6, chalcopyrite [$CuFeS_2$], pentlandite [$(Fe, Ni)_9S_8$], tausonite [SrTiO3], Ferropericlase [(Mg, Fe)O], calcite [$CaCO_3$], breyite [CaSiO3], and enstatite [(MgSiO3)]) were identified; an assembly of typically found in sub-lithospheric mineral inclusions ac-

cording to what can be seen in Hutchison (1997); Harte and Hudson (2014); Kaminsky (2017); Shirey and Wagner (2021); Walter *et al.* (2022); Smith (2018); Smith *et al.* (2022); Nestola (2017); Litvin (2017) Spivak and Litvin (2019).

An assembly typically found in sub-lithospheric diamond inclusions; i.e. ferropericlase and breyite (*cf.* Litvin, 2017; Spivak and Litvin, 2019; Kaminsky, 2017; and Walter *et al.*, 2022) was also identified in others Capiibary diamond samples (Capii-16 and Capii-17) (Figure 4). Though the Raman peak of ferropericlase is more prominent in the sample Capii-6 than in Capii-16 and Capii-17 (Figure 4C).

Stishovite [SiO_2] inclusion along with corundum [Al_2O_3] is identified in sample Capii-7 (multiple inclusion, Figure 5), which also supports the notion of probable sub-lithospheric origin (*cf.* Litvin, 2017; Spivak and Litvin, 2019; Kaminsky, 2017) of the studied diamonds.

Inclusions of corundum are also identified in samples Capii-10 and Capii-14. The Raman spectrum of Capii-14 also shows stishovite peaks; as already commented, a member of the minerals phase that is typical of sub-lithospheric diamond inclusions suit.

Juina-like perovskite [$CaTiO_3$] inclusion is highlighted in Figures 7 (A and B), which was identified in sample Capii-1. The Raman spectrum of Capii-1 perovskite (Figure 7C, Table 1) shows four well-individualized peaks that are compared to the Juina super deep perovskite inclusion Raman spectrum

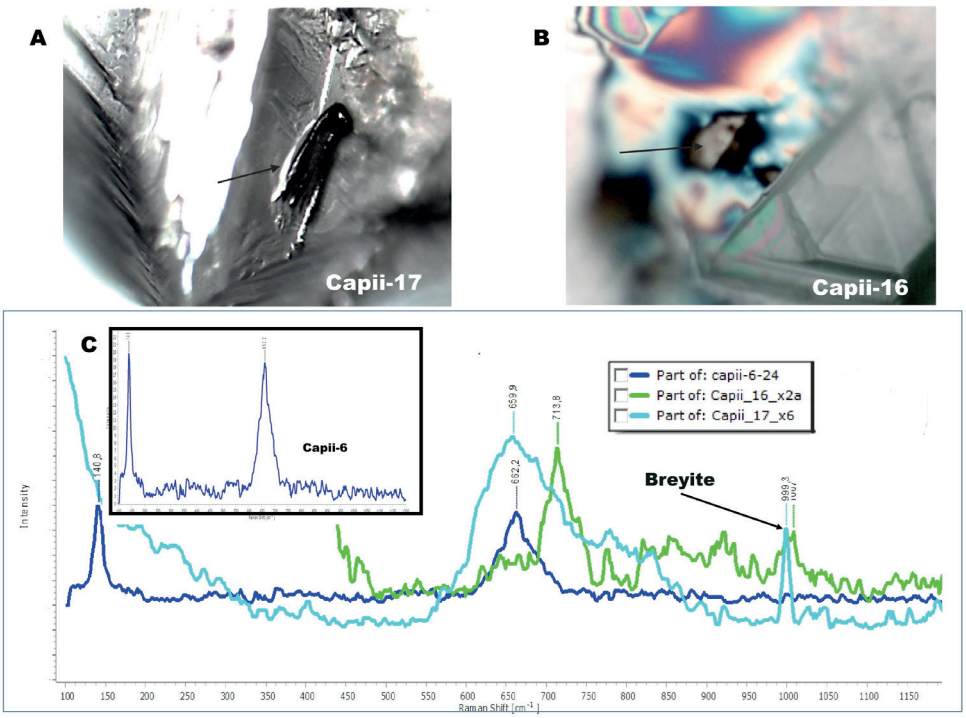

Figure 4 - Photomicrograph of ferropericlase inclusion in Capii-16 (A) and Capii-17 (B) and the Raman spectrum where ferropericlase is identified (C) in samples Capii-6, Capii-16, and Capii-17. The highlighted ferropericlase peaks in box one that is obtained from Capii-6. In Capii-17 the spectrum is of multiple inclusion of ferropericlase with breyite.

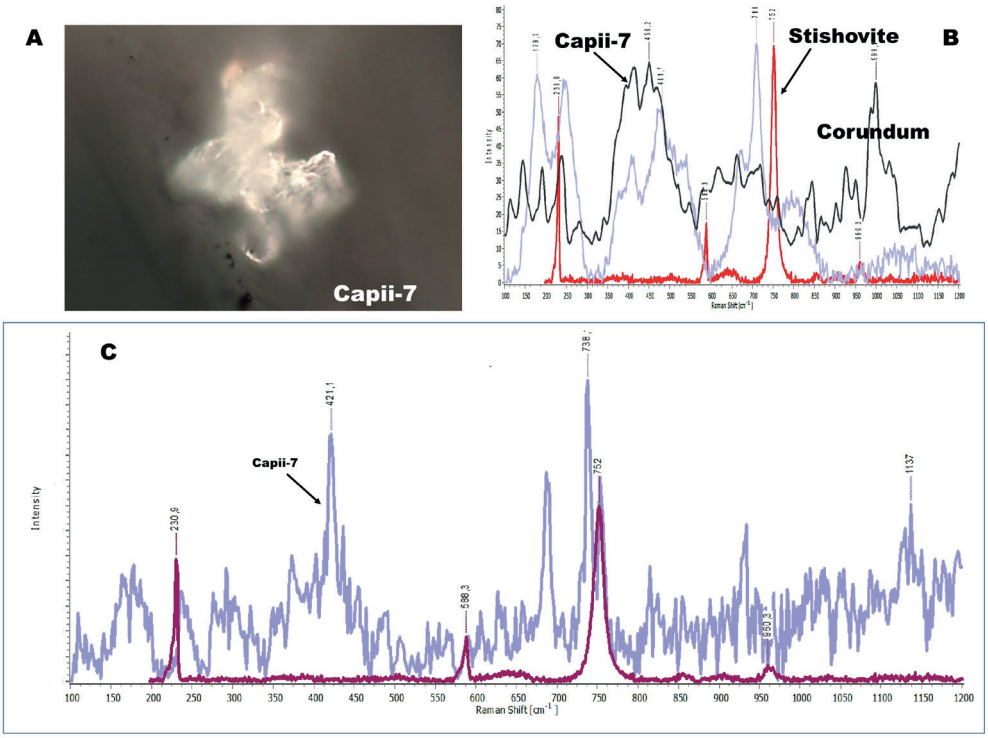

Figure 5 - A. Photomicrograph of stishovite inclusion in Capii-7 and the Raman spectrum. B. multiple inclusion spectra (corundum and stishovite) contrasted with stishovite pattern (red color); and stishovite spectra of Capii-7 with corundum (compared with the Raman spectrum of corundum that would be the retrograde product of bridgmanite) and stishovite source spectra from Smith (2021).

(from Smith, 2021) is at the same time both different from Ca-pv ($CaSiO_3$) Raman spectrum of Nestola *et al.* (2018); this when the comparison is extended from 100 to 1300 cm^{-1} Raman shift. The slightly higher shift of the Capii-1 perovskite peaks would be due to a higher formation pressure as could be interpreted from what is shown by Shim *et al.* (2007).

The results of mineral inclusions identification by confocal Raman spectroscopy from 11 selected diamond samples are summarized in Table 1. But the Raman spectroscopy alone cannot interpret precisely the original inclusion mineralogy due to multiple high phases of mineral inclusions trapped together in the diamonds due to retrogression (Smith *et al.*, 2022).

Yet, in summary, the mineral inclusions identified in the 11 selected Capiibary diamonds by Raman spectroscopy were: pentlandite $[(Ni_xFe_y)_{\Sigma 9}S_8]$, chalcopyrite $[CuFeS_2]$, and molybdenite $[MoS_2]$, calcium-silicate (larnite $[Ca_2SiO_4]$, breyite $[CaSiO_3]$, and wollastonite $[Ca_3(Si_3O_9)]$, merwinite $[Ca_3Mg(SiO_4)_2]$, corundum $[Al_2O_3]$-enstatite (or retrogression bridgmanite [(Mg, Fe) SiO_3] maybe Al-bearing; i.e., former $MgSiO_3$-perovskite: mPv); stishovite $[SiO_2]$, ferropericlase [(Mg,Fe)O]; nepheline $[NaAlSiO_4]$ and spinel $[Mg,Fe)Al_2O_4]$, Ca-perovskite [Juina like $CaTiO_3$], calcite, graphite, and tausonite $[SrTiO_3]$ (Table 1). And to them is added the assembly of inclusions of peridotitic affinity magnesiochromite $[MgCr_2O_4]$; diopside $[CaMgSi_2O_6]$

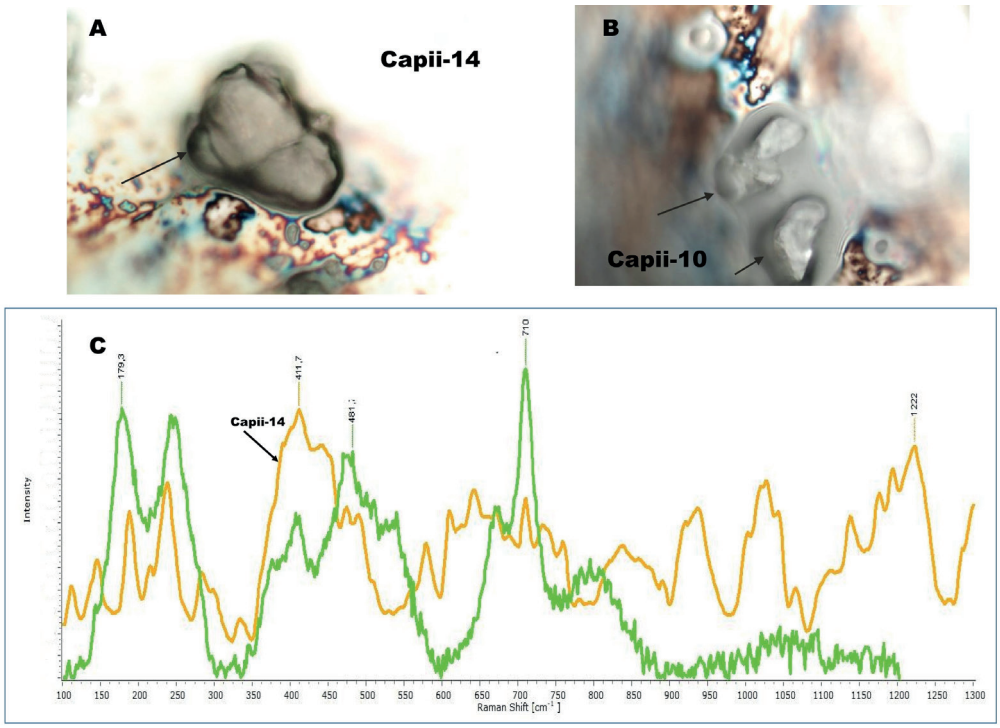

Figure 6 - Photomicrograph of corundum inclusion in Capii-14 (A) and Capii-10 (B) and the corresponding Raman spectrum (multiple inclusion with corundum that would be the retrograde product of bridgmanite, (Smith, 2021).

and perovskite in the diamond Capii-2. (Table 1).

Corundum and enstatite are interpreted as probable products of retrogression of the bridgmanite (former MgSiO3-perovskite). And so; Calcium-silicate minerals are seen as formed from retrogression of the Ca-perovskite. Nephelinte+spinel is interpreted as a probable product of the retrogression of CF phase (calcium ferrite). Inclusions that are commonly interpreted to represent high-pressure phases with a former 'perovskite' structure that have retrogressed to lower-pressure polymorphs or phase assemblages (*cf*. comments, for example, in Hutchison, 1997; Walter *et al*., 2022; Smith *et al*., 2022).

The Ca-perovskite ($CaTiO_3$) to retrogression Ca-perovskite ($CaSiO_3$) and retrogression bridgmanite, stishovite, and ferropericlase inclusion associations would seem to be the suite of mineral inclusions in the selected Capiibary diamonds (Table-1) and suggest sub-lithospheric diamonds inclusion; i.e., bridgmanite-cPv-stishovite-CF association (based in Harte and Hudson, 2014; Litvin, 2017; Spivak and Litvin, 2019; Kaminsky, 2017). The cratonic mantle of peridotitic affinity inclusion is recognized in a single diamond crystal (Capii-2). The carbonate and merwinite inclusions in the Capiibary diamonds probably formed from carbonatitic components in the lower mantle (*cf*. Litvin 2017; Spivak and Litvin, 2019; Kaminsky, 2017).

CONCLUSIONS

In Eastern Paraguay, only Mesozoic (Ju-

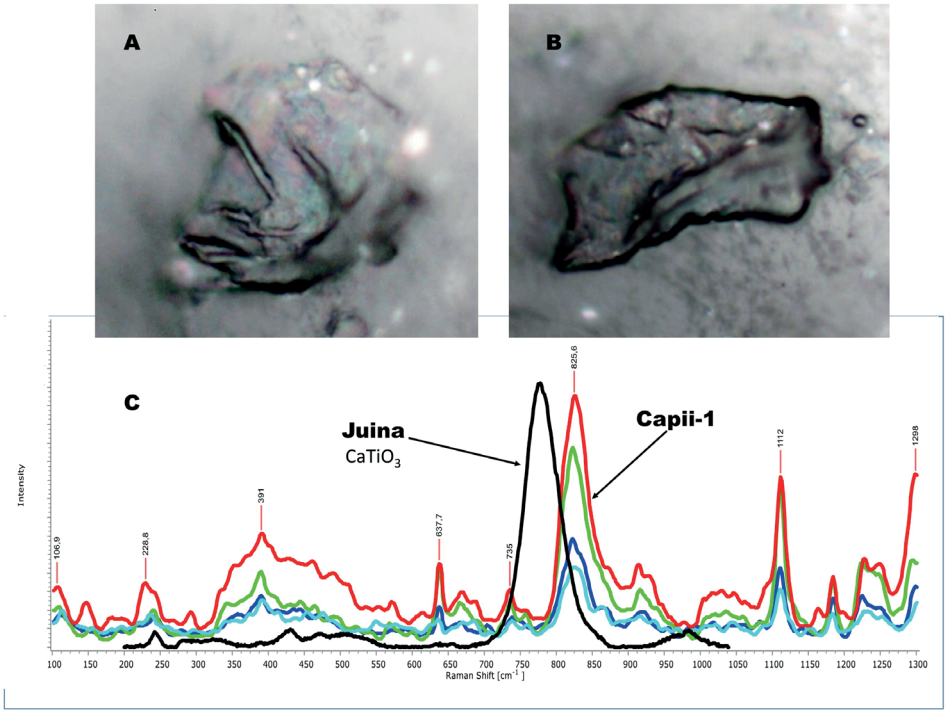

Figure 7 - Juina-like perovskite [$CaTiO_3$] inclusion (7A and B) was identified in sample Capii-1. The Raman spectrum of Capii-1 perovskite (7C) is similar to the super deep Juina perovskite Raman spectrum [$CaTiO_3$] (Smith, 2021) and so is the super pressure perovskite Raman spectrum of Shim *et al.* (2007).

rassic/Cretaceous) cratonic diamond-bearing lamproites would occur in numerous fields (*cf*. Presser, 2016; Presser, 2019a-b; Presser *et al*., 2014 Presser *et al*., 2017). One of these fields is next to the city of Capiibary (Department of San Pedro). After previous studies in Capiibary diamonds carried out by Smith *et al.* (2014) and extensively developed by Presser *et al.* (2014b); this work focused on studying a new batch of 22 diamonds (alluvial/colluvial from a lamproitic pipe anomaly). The present study was based above all on the study by Raman spectroscopy of the structure of 11 selected diamonds and the determination of the inclusions in them.

The spectral characteristics of the Capiibary diamonds, as revealed from the present study, are quite different from the defect-free cubic natural diamonds, in terms of the intensity and the value of the D-band (peak wavenumber 1294 to 1353 cm^{-1}), the value of FWHM (>>3 to 197 cm^{-1}) that indicate the presence of the lonsdaleite component in the Capiibary diamonds (i.e.; lonsdaleitic diamonds). The formation of lonsdaleite requires a formation pressure greater than 30 Gpa. (*cf*. He *et al*., 2002 and DeCarli *et al*., 2002); that is, most likely in areas of the lower mantle. Moreover, the assembly of mineral inclusions identified in most of the diamonds, that are extensively recognized by Raman spectroscopy, were indicated to be: sulfides (pentlandite, chalcopyrite, and molybdenite); calcium-silicate (larnite, breyite, and wollastonite); merwinite, stishovite; ferropericlase; CF phase; Ca-perovskite; enstatite-corundum; calcite; graphite; and tau-

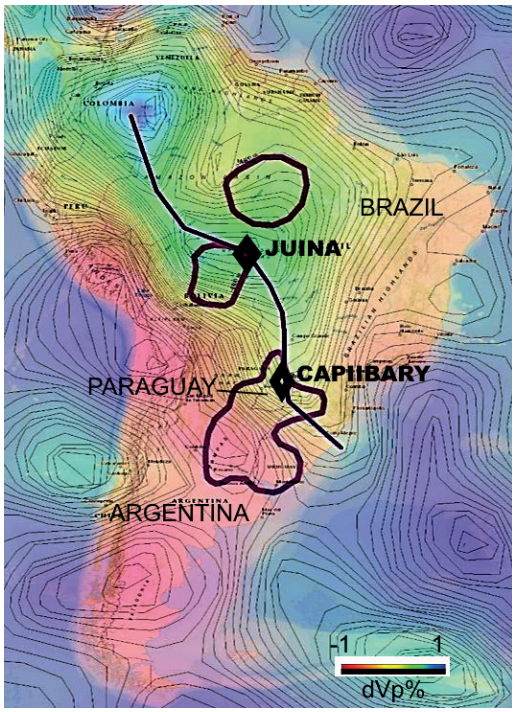

Figure 8 - Position of the Nazca Plate at a depth of 1075 km (highlighting the approximate midpoint according to the line drawn above in the high-velocity dVp zone) based on data from TX2019slab (Lu *et al.*, 2019) that could be extracted from http://ds.iris.edu/ (September 2022). It is estimated that the Capiibary diamonds and the Juina diamonds would share the same source of their super deep diamonds; I.e., the Nazca slab which seems at this depth to have overflowed as irregular and wide (plastic?) mass. The areas enclosed in purple lines correspond to the Archon cratonic blocks (Presser and Benitez, 2021 and references).

sonite (Figures 3, 4, 5, 6 and 7, and Table 1). The mineral inclusions are considered reliable indicator minerals for the native matter of the lower mantle (as can be read in Litvin, 2017; Spivak and Litvin, 2019; Kaminsky, 2017; Walter *et al.*, 2022). In a nutshell Ca-perovskite to retrogression-perovskite and retrogression bridgmanite, stishovite, and ferropericlase inclusion associations (Table 1); i.e. sub lithospheric basic (composition) lower mantle diamonds-hosted inclusions (*cf.* Spivak and Litvin, 2019; Kaminsky, 2017, and also Harte and Hudson, 2014).

The discovery of the experimental mechanism of the formation of hexagonal diamond due to a direct solid-to-solid transition within cubic diamond by a kinetic process of shear stress and high temperature induced by the shock wave compression (He *et al.*, 2002); supports the theoretical possibility of the formation of diamonds in the subducted slab at depths below the transition zone and/or lower mantle could be transformed partially into lonsdaleite diamonds or mixed cubic and hexagonal polytype structures of diamonds (*cf.* Kaminsky and Voropaev, 2021; Shirey *et al.*, 2021; Gorshkov *et al.*, 1997; Kaminsky, 2017; Wu *et al.*, 2020).

The subtle component lonsdaleite along with the sub-lithospheric suite of mineral inclusion in Capiibary diamonds can be explained as that the diamond traveled downward dragged down by a subducting slab (Figure 8) in the lower mantle, before being delivered to the surface; positioned as previously supposed by Lorenzon *et al.* (2022) for the super deep diamond's inclusions from the Central African Republic. So, the Capiibary diamonds would have transformed partially into lonsdaleite or mixed cubic hexagonal polytype structures of diamonds by a kinetic process of shear stress and the shock wave compression induced by provable very high temperature.

ACKNOWLEDGMENT

The authors are grateful to the technician in diamond geology of the city of Capiibary Rodolfo Gavilán for the meticulous selection of the diamonds for the present study. The authors are also grateful to Dr. Dmitry Pestov and Dr. Carl Mayer for their support in Micro Raman Analysis at NCCF of Virginia Commonwealth University (VCU), USA.

Table 1 - Diamond ID, Inclusions, number of spectra obtained per crystal, and probable origin according to the assemblage of mineral inclusions.

Diamond ID Diamond Raman Spectra data	Inclusions	Nº of Raman Spectra	Probable Deep Origen
Capii-1 Raw Peak wavenumber: 1294-1331.8 cm^{-1} FWHM: 4.6-306 cm^{-1}	Pentlandite, tausonite, nepheline (retrograde CF phase), perovskite ($CaTiO_3$), corundum (former bridgmanite)	38	Lower Mantle Ass: Ca-Perovskite-bridgmanite-CF phase Lonsdaleitic diamond: Peak wavenumber: 1294.1-1331.8 cm^{-1} FWHM Baseline:4.3-76 cm^{-1}
Capii-2 Raw Peak wavenumber: 1330.8-1332.3 cm^{-1} FWHM: 4.3-9.96 cm^{-1}	Magnesiochromite, diopside, perovskite	19	Peridotitic lithospheric diamond
Capii-3 Raw Peak wavenumber: 1330.1-1334.7 cm^{-1} FWHM: 4.6-281 cm^{-1}	Merwinite, corundum (former bridgmanite)	17	Lower Mantle Ass: Bridgmanite-merwinite Lonsdaleitic diamond: Peak wavenumber: 1330-1332.1 cm^{-1} FWHM Baseline:5.4-63 cm^{-1}
Capii-5 Raw Peak wavenumber: 1330.7-1331.7 cm^{-1} FWHM: 5.1-6.8 cm^{-1}	Molibdenite, larnite (former Ca-perovskite)	10	? Transition zone/ Lower Mantle Ass: **cPv** Lonsdaleitic diamond: Peak wavenumber: 1326.3-1331.7 cm^{-1} FWHM Baseline: 4.96-24.3 cm^{-1}
Capii-6 Raw Peak wavenumber: 1315.6-1353.4 cm^{-1} FWHM: 4.3-194.7 cm^{-1}	Chalcopyrite, pentlandite, tausonite, periclase, breyite-wollastonite (former Ca-perovskite), calcite, enstatite (former bridgmanite)	42	Lower Mantle Ass: Bridgmanite-Periclase-cPv-calcite Lonsdaleitic diamond: Peak wavenumber: 1313.4-1353.4 cm^{-1} Lonsdaleitic diamond: FWHM Baseline:2.32-197 cm^{-1}
Capii-7 Raw Peak wavenumber: 1329.3-1331.1 cm^{-1} FWHM: 4.0-513.8 cm^{-1}	Chalcopyrite, tausonite, breyite (former Ca-perovskite), nepheline+spinel (retrograde CF phase), stishovite, corundum, and enstatite (both former bridgmanite)	25	Lower Mantle Ass: cPv-Bridgmanite-stishovite-CF Lonsdaleitic diamond: baseline peak wavenumber:1329-1347 cm^{-1} FWHM Baseline: 9-68.3 cm^{-1}
Capii-8 Raw Peak wavenumber: 1330.9-1333.6 cm^{-1} FWHM: 4.2-10.9 cm^{-1}	Pentlandite-, corundum, and enstatite (both former bridgmanite), nepheline+spinel (retrograde CF phase), periclase	6	Lower Mantle Ass: Bridgmanite-periclase-CF
Capii-10 Raw Peak wavenumber: 1331.1-1331.7 cm^{-1} FWHM: 5-93 cm^{-1}	Corundum and enstatite (both former bridgmanite),? nepheline (retrograde CF phase)	6	Lower Mantle Ass: Brigmanite—CF Lonsdaleitic diamond: baseline peak wavenumber:1331.1-1331.7 cm^{-1} FWHM Baseline: 9-22 cm^{-1}
Capii-14 Raw Peak wavenumber: 1330.1-1331.3 cm^{-1} FWHM: 4.1-700 cm^{-1}	Stishovite, enstatite, and corundum (both former bridgmanite)	18	Lower Mantle Ass: Brigmanite-Stishovite Lonsdaleitic diamond: baseline peak wavenumber:1330.1-1331.2 cm^{-1} FWHM Baseline: 9-42.5 cm^{-1}
Capii-16 Raw Peak wavenumber: 1328.8-1331.6 cm^{-1} FWHM: 4.6-82.9 cm^{-1}	Periclase, nepheline (retrograde CF phase), breyite (former Ca-perovskite), enstatite (former bridgmanite) Brigmanite-cPv-periclase	11	Lower Mantle Ass: Brigmanite-cPv-periclase Lonsdaleitic diamond: baseline peak wavenumber:1328.6-1329.6 cm^{-1} FWHM Baseline: 9.1-10.3 cm^{-1}
Capii-17 Raw Peak wavenumber: 1328.9-1329.9 cm^{-1} FWHM: 4.3-402 cm^{-1}	Periclase, nepheline (retrograde CF phase), breyite (former Ca-perovskite), enstatite (former bridgmanite)	8	Lower Mantle Ass: Brigmanite-cPv-periclase¨-CF Lonsdaleitic diamond: baseline peak wavenumber:1329.2-1331.6 cm^{-1} FWHM Baseline: 9.2-10.3 cm^{-1}

REFERENCES

Anzolini, C. Prencipe, M. Alvaro, M. Romano, C. Vona, A. Lorenzon, S. Smith, E.M. Brenker, F.E. and Nestola, F. (2018). Depth of formation of super-deep diamonds: Raman barometry of $CaSiO_3$-breyite inclusions. Am. Mineral 103:69–74.

DeCarli, P.S. Bowden, E. Jones, A.P. and Price, G.D. (2002). Laboratory impact experiments versus natural impact events. Geological Society of America Special Paper 356, 59.

Di Liscia, E. J. Álvarez, F. Burgos, E. Halac, E. B. Huck, H. and Reinoso, M. (2013). Stress Analysis on Single-Crystal Diamonds by Raman Spectroscopy 3D Mapping. *Materials Sciences and Applications*, 4, 191-197.

Green, B.L Collins, A.T. and Breeding, Ch.M. (2022). Diamond Spectroscopy, Defect Centers, Color, and Treatments. Reviews in Mineralogy & Geochemistry: Vol. 88 pp. 637–688.

Gorshkov, A.I. Yanan, B. Bershov, L.V. Ryabchikov, I.D. Sivtsov, A. and Lapina, V. (1997). Inclusions in diamond from the Liaoning Deposit (China) and their genetic meaning. Geochemistry International 35, 58-65.

Goryainov, S. V. Likhacheva, A. Y. Rashchenko, S. V. Shubin, A. S. Afanas'ev, V. P. and Pokhilenko, N. P. J. (2014). Raman identification of lonsdaleite in Popigai Impactites. J. Raman Spectrosc. Wiley on linelibrary. com/journal/jrs.

Harte, B. and Hudson, N.F.C. (2013). Mineral Associations in Diamonds from the Lowermost Upper Mantle and Uppermost Lower Mantle. In: D. G. Pearson et al. (eds.), Proceedings of 10th International Kimberlite Conference, Volume 1, Special Issue of the Journal of the Geological Society of India, 235-253.

He, H. Sekine, T. and Kobayashi, T. (2002). Direct transformation of cubic diamond to hexagonal diamond. Appl. Phys. Lett., Vol. 81, No. 4: 610-612.

Hutchison, M. T. (1997). Constitution of the deep transition zone and lower mantle shown by diamonds and their inclusions (Unpublished Ph.D. thesis). University of Edinburgh, UK. Vol. 1, 340 pp., Vol. 2 (Tables and Appendices), 306 pp.

Jones, A.P. McMillan, P.F Salzmann, Sh.G. Alvaro, M. Nestola, F. Prencipe, M. Dobson, D. Hazael, R. and Moore, M. (2016). Structural characterization of natural diamond shocked to 60 GPa; implications for Earth and planetary systems. Lithos 265, 214–221.

Kaminsky, F.V. (2017). Earth's Lower Mantle: Composition and Structure. Springer Geology, 331 pp.

Kaminsky, F.V. and Voropaev, S.A. (2021). Modern Concepts on Diamond Genesis. Geochemistry International, Vol. 59, No. 11, pp. 1038–1051.

Kemppinen, L.I.M. (2019). Investigating the timing and nature of diamond-forming events through the study of diamond-hosted sulphide inclusions. Thesis (Ph.D.) University of Bristol. ISN:0000000493470764.

Litvin Y.A. (2017). Genesis of diamonds and associated phases. Springer, 137 p.

Lorenzon, S. Novella, D. Nimis, P. Jacobsen, S. D. Thomassot, E. Pamato, M.G. Prosperi, L. Lorenzetti, A. Alvaro, M. Brenker, Fr. Salvadego, Fr. and Nestola, F. (2022). Ringwoodite and zirconia inclusions indicate downward travel of super-deep diamonds. Geology, v. XX, p. XXX.

Lu, C. Grand, S. P. Lai, H. and Garnero, E. J. (2019). TX2019slab: A new P and S tomography model incorporating subducting slabs. Journal of Geophysical Research: Solid Earth, 124, 11,549–11,567.

Miyamoto, M. Takase, T. and Mitsuda, Y. (1993). Raman spectra of various diamonds. Mineral. J., 16, 246-257.

Murri, M. Smith, R.L. McColl, K. Hart, M. Alvaro, M. Jones, A.P. Németh, P. Salzmann, Chr. G. Corà, F. Domeneghetti, M. C. Nestola, F. Sobolev, N.V. Vishnevsky, S. A. Logvinova, A. M and McMillan, P. F. (2019). Quantifying hexagonal stacking in Diamond. Scientific Reports 9, 10334.

Németh, P. Lancaster, H.J. Salzmann, C.G. McColl, K. Fogarassy, Z. Garvie, L.A.J. Illés, L. Pécz, B. Murri, M. Corà, F. Smith, R.L. Mezouar, M. Howard, C.A. and McMillan, P.F. (2022). Shock-formed carbon materials with intergrown sp^3- and sp^2-bonded nanostructured units. Proc Natl Acad Sci U S A., 26;119 (30).

Nestola, F. (2017). Inclusions in super-deep diamonds: windows on the very deep Earth. Rend Lincei-Mat Appl 28:595–604.

Nestola, F. N. Korolev, N. Kopylova, M. Rotiroti, N. Pearson, D. G. Pamato, M. G. Alvaro, M. Peruzzo, L. Gurney, J. J. Moore, A. E. and Davidson, J. (2018). $CaSiO_3$ perovskite in diamond indicates the recycling of oceanic crust into the lower mantle. VOL 555| Nature| 237.

Ovsyuk, N.N. Goryainov, S.V. and Likhacheva, A.Y. (2019). Raman scattering of impact diamonds, Diamond and Related Materials, Volume 91: 207-212.

Presser, J.L.B. (2016). Diamantes en Paraguay, Cincuenta Años de Ocurrencia. Bol. Mus. Nac. Hist. Nat. Parag. Vol. 20, nº 2: 154-187.

Presser, J.L.B. (2019a). Diamonds occurrences in Paraguay. Paraguay, Diamond Deposits Exploration Event DDEE, Asunción. Paraguay.

Presser, J.L.B. (2019b). El lamprófido picrítico con diamantes Ymi-1. Pyroclastic Flow, 9(1): 23-34.

Presser, J.L.B., Bitschene, P. R. and Vladykin, N.V. (2014a). Comentarios Sobre La Geología, La Petrografía y La Química Mineral De Algunas Lamproítas De La Porción Norte De La Cordillera Del Ybytyruzú, Paraguay Oriental. Bol. Mus. Nac. Hist. Nat. Parag. 18(1): 24-61.

Presser, J.L.B. Bulanova, G.P. and Smith, C.B. (2014b). Diamantes De Capiibary, Dpto. San Pedro, Paraguay. Boletin del Museo Nacional de Historia Natural del Paraguay, 18(1): 5-23.

Presser, J.L.B., Vladykin, N.V., Bitschene, P.R., Tondo, M. J., Acevedo, R.D., Alonso, R. and Benitez, P. (2017). Olivino-lamproita del Campo de Lamproitas Ybytyruzú, Paraguay Oriental. Pyroclastic Flow, 7 (1): 1-15.

Presser, J.L.B. Monteiro, M. and Maldonado, A. (2020). Impact diamonds in an extravagantmetal piece found in Paraguay. Historia Natural Tercera Serie Volumen 10 (2) 5-15.

Presser, J.L.B. and Benítez, P. (2021). Geophysical constraints of the Rio de la Plata's Archon Craton. Historia Natural. Tercera Serie Volumen 11 (2) 2020/17-37.

Qiu, W. Velisavljevic, N. Baker, P. A. Vohraa, Y. K. and Weir, S. T. (2004). Isotopically pure 13^{C} layer as a stress sensor in a diamond anvil cell. Applied physics letters. Volume 84 (26).

Shirey, S. B. Wagner, L. S. Walter, M. J. Pearson, D.G. and van Keken, P. E. (2021). Slab transport of fluids to deep focus earthquake depths—thermal modeling constraints and evidence from diamonds. AGU Advances, 2, e2020AV000304.

Shim, S.-H. Kubo, A. and Duffy, T.S. (2007). Raman spectroscopy of perovskite and post-perovskite phases of $MgGeO_3$ to 123 GPa. Earth and Planetary Science Letters 260: 166–178.

Smith, C.B. Bulanova, G.P. and Presser, J.L.B. (2012). Diamonds from Capiibary, Paraguay. 10th International Kimberlite Conference Extended Abstract No. 10IKC-36.

Smith, E.M. (2021). Raman spectra catalogue for inclusions in diamond. https://doi.org/10.7939/DVN/JEHGBW.

Smith, E.M. Shirey, S.B. and Wuyi, W. (2017). The very deep origin of the world's biggest diamonds. Gems & Gemology, Winter 2017, Vol. 53, No.4.

Smith, E.M. Shirey, S.B. Richardson, S.H. Nestola, F. Bullock, E.S. Wang, J. and Wang, W. (2018). Blue boron-bearing diamonds from Earth's lower mantle. Nature 560:84–87.

Smith, E. Krebs, M.Y. Genzel, P-T. and Brenker, F.E. (2022). Raman Identification of Inclusions in Diamond. Reviews in Mineralogy & Geochemistry 8 Vol. 88 pp. 451-474.

Spivak, A.V. and Litvin, Y.A. (2019). Evolution of Magmatic and Diamond-Forming Systems of the Earth's Lower Mantle. Springer, 103 p.

Thomson, A. R. Kohn, S. C. Bulanova, G. P. Smith, C. B. Araujo, D. and Walter, M. J. (2014). Origin of sub-lithospheric diamonds from the Juina-5 kimberlite (Brazil): Constraints from carbon isotopes and inclusion compositions. Contributions to Mineralogy and Petrology,168, 1081.

Walter, J. M. Thomson R.A. and Smith, E.M. (2022). Geochemistry of Silicate and Oxide Inclusions in Sublithospheric Diamonds. Reviews in Mineralogy & Geochemistry 7 Vol. 88 pp. 393-450.

Wu, G.-C. Yu, X.-Y Liu, F. Li, H.-B. Long, Z.-Y. and Wang, H. (2022). Color Genesis of Brown Diamond from the Mengyin Kimberlite, China. *Crystals* 12.

Zaitsev, A.M. (2013). Optical properties of diamond: A data handbook. Springer Science and Business Media.

Zedgenizov, D.A. Ragozin, A. L. Kalininaa, V.V. and Kagi, H. (2016). The mineralogy of Ca-rich inclusions in sublithospheric diamonds. Geochemistry International, 54 (10), 890–900.

Zedgenizov, D.A. Kagi, H. Ohtani, E. Tsujimori, T. and Komatsu, K. (2020). Retrograde phases of former bridgmanite inclusions in superdeep diamonds, Lithos, Vol. 370–371.

Recibido: 13/04/2022 - Aceptado: 17/11/2022 -Publicado: 18/01/2023